

# Communications

## Novel 5 V Spinel Cathode $\text{Li}_2\text{FeMn}_3\text{O}_8$ for Lithium Ion Batteries

Hiroo Kawai,<sup>†</sup> Mikito Nagata,<sup>‡</sup>  
Mitsuharu Tabuchi,<sup>§</sup> Hisashi Tukamoto,<sup>‡</sup> and  
Anthony R. West<sup>\*†</sup>

Department of Chemistry, University of Aberdeen,  
Meston Walk, Aberdeen AB24 3UE,  
Scotland, United Kingdom,  
Corporate R&D Center,  
Japan Storage Battery Company Limited,  
Nishinosho, Kisshoin, Minami-ku, Kyoto 601, Japan,  
and Osaka National Research Institute,  
1-8-31 Midorigaoka, Ikeda, Osaka 563, Japan

Received May 11, 1998

$\text{LiCoO}_2$ <sup>1</sup> is the first cathode material to be used in commercial lithium ion rechargeable cells<sup>2</sup> and operates at  $\sim 3.7$  V vs  $\text{Li/Li}^+$ . A recent approach to improved cathode materials has been to replace expensive and toxic  $\text{LiCoO}_2$  by the 3.8 V cathode  $\text{LiMn}_2\text{O}_4$ <sup>3–5</sup> in state-of-the-art cells.<sup>6</sup> These cells can successfully substitute for conventional systems such as nickel–cadmium in portable electronic devices,<sup>7</sup> but larger scale batteries for zero-emission vehicles require further improvement in energy density by either increasing capacity or raising operating voltage. Cells with cathode materials  $\text{LiMnO}_2$ <sup>8</sup> and  $\text{Li}_{1.5}\text{Na}_{0.5}\text{Mn}_{0.85}\text{I}_{0.12}$ <sup>9</sup> exhibited higher capacity, but the former needs improved cycling stability and the latter would require higher working voltage. Cells with cathode materials based on spinel structure compounds and improved electrolytes<sup>10</sup> showed higher operating voltages: 4.8 V for  $\text{LiNiVO}_4$ <sup>11,12</sup> and  $\text{LiCr}_x\text{Mn}_{2-x}\text{O}_4$ <sup>13,14</sup> and 4.7 V for  $\text{LiNi}_x\text{Mn}_{2-x}\text{O}_4$ .<sup>15–17</sup> We recently reported

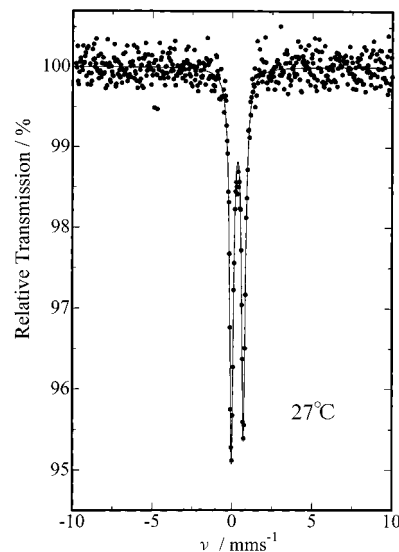


Figure 1. <sup>57</sup>Mössbauer spectrum for  $\text{Li}_2\text{FeMn}_3\text{O}_8$ .

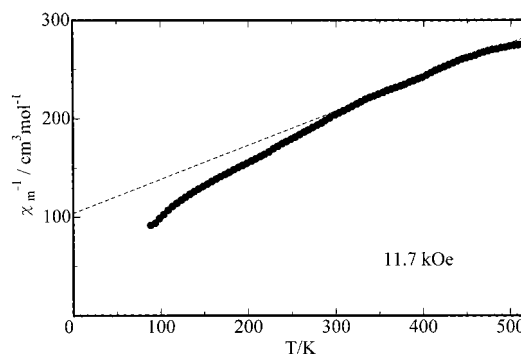


Figure 2. Magnetic susceptibility data for  $\text{Li}_2\text{FeMn}_3\text{O}_8$ .

the spinel  $\text{Li}_2\text{CoMn}_3\text{O}_8$ , the first cathode material operating over 5 V.<sup>18</sup> Here we report a new 5 V cathode material,  $\text{Li}_2\text{FeMn}_3\text{O}_8$ ; this is the first high-voltage system to contain substantial Fe content and offers potential economical and environmental advantages.

A phase-pure sample of  $\text{Li}_2\text{FeMn}_3\text{O}_8$  was prepared by conventional solid-state synthesis: a stoichiometric mixture of dried  $\text{Li}_2\text{CO}_3$ ,  $\text{MnCO}_3$ , and undried  $\text{FeC}_2\text{O}_4 \cdot 2\text{H}_2\text{O}$ , all reagent grade, was ground intimately and fired under oxygen flow, initially at 650 °C for 2 h to drive off  $\text{CO}_2$  and then at 750 °C for 3 days with intermittent regrinding, followed by slow-cooling to room temperature. An <sup>57</sup>Fe Mössbauer spectrum was measured for the as-prepared sample with a Toyo Research FGX-100S apparatus, <sup>57</sup>Co source, using the spectrometer velocity ( $\nu$ ) scale calibrated with  $\alpha$ -Fe. The

<sup>†</sup> University of Aberdeen.

<sup>‡</sup> Japan Storage Battery Company Limited.

<sup>§</sup> Osaka National Research Institute.

(1) Mizushima, K.; Jones, P. C.; Wiseman, P. C.; Goodenough, J. B. *Mater. Res. Bull.* **1980**, *15*, 783.

(2) Nagaura, T.; Tozawa, K. *Prog. Batteries Sol. Cells* **1990**, *9*, 209.

(3) Ohzuku, T.; Kitagawa, M.; Hirai, T. *J. Electrochem. Soc.* **1990**, *137*, 769.

(4) Tarascon, J. M.; Wang, E.; Shokoohi, F. K.; McKinnon, W. R.; Colson, S. *J. Electrochem. Soc.* **1991**, *138*, 2859.

(5) Yamada, A.; Miura, K.; Hinokuma, K.; Tanaka, M. *J. Electrochem. Soc.* **1995**, *142*, 2149.

(6) Japan Electronics, March 6th, **1996**.

(7) JEC Battery Newsletter, Sony Corporation Battery Group and Sony Energytec, July–August, **1993**, p 19.

(8) Armstrong, A. R.; Bruce, P. G. *Nature* **1996**, *381*, 499.

(9) Kim, J.; Manthiram, A. *Nature* **1997**, *390*, 265.

(10) Tarascon, J. M.; Guyomard, D. *Solid State Ionics* **1994**, *69*, 293.

(11) Fey, G. T.-K.; Li, W.; Dahn, J. R. *J. Electrochem. Soc.* **1994**, *141*, 2279.

(12) Prabaharan, S. R. S.; Michael, M. S.; Radhakrishna, S.; Julien, C. *J. Mater. Chem.* **1997**, *7*, 1791.

(13) Sigala, C.; Guyomard, D.; Verbaere, A.; Piffard, Y.; Tournoux, M. *Solid State Ionics* **1995**, *81*, 167.

(14) Sigala, C.; Verbaere, A.; Mansot, J. L.; Guyomard, D.; Piffard, Y.; Tournoux, M. *J. Solid State Chem.* **1997**, *132*, 372.

(15) Amine, K.; Tukamoto, H.; Yasuda, H.; Fujita, Y. *J. Electrochem. Soc.* **1996**, *143*, 1607.

(16) Zhong, Q.; Bonakdarpour, A.; Zhang, M.; Gao, Y.; Dahn, J. R. *J. Electrochem. Soc.* **1997**, *144*, 205.

(17) Gao, Y.; Myrtle, K.; Zhang, M.; Reimers, J.; Dahn, J. R. *Phys. Rev. B* **1996**, *54*, 16670.

(18) Kawai, H.; Nagata, M.; Tukamoto, H.; West, A. R. *J. Mater. Chem.* **1998**, *8*, 837.

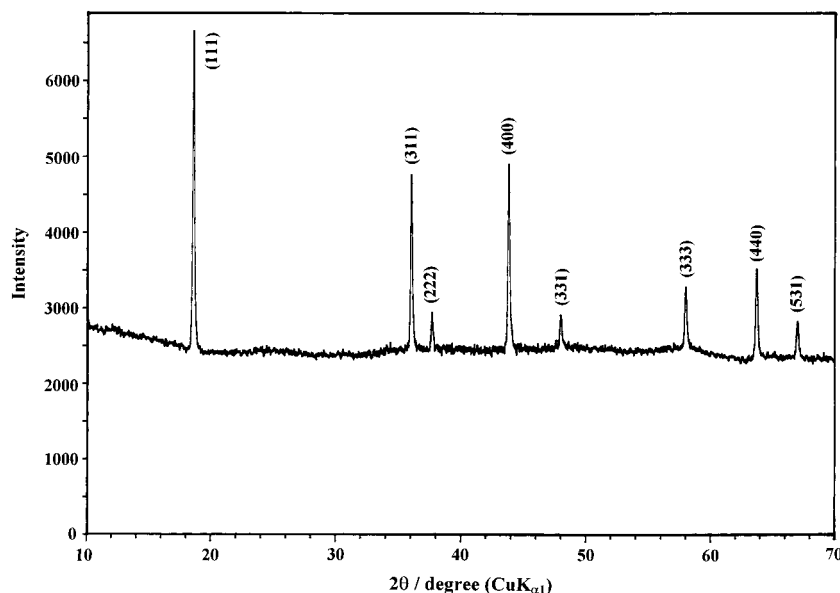


**Figure 3.** Powder XRD profile for  $\text{Li}_2\text{FeMn}_3\text{O}_8$ .

sharp, symmetrical doublet observed implies that all Fe has the same valence state and occupies crystallographically the same site (Figure 1). The estimated isomer shift,  $+0.35$  mm/s, is characteristic of high-spin  $\text{Fe}^{3+}$ . Magnetic susceptibility data were recorded in the temperature range 83–513 K, with a MB-3 Shimadzu Faraday balance, using Tutton's salt,  $(\text{NH}_4)_2\text{Mn}(\text{SO}_4)_2 \cdot 6\text{H}_2\text{O}$  as a reference. Above 300 K, the magnetic molar susceptibility,  $\chi_m$ , fits the Curie–Weiss law,  $\chi_m^{-1} = (T - \theta)/C$ , where  $\theta$  is the Weiss constant and  $C$  is a constant (Figure 2). Effective magnetic moment per paramagnetic ion, i.e.,  $\text{Fe}_{1/4}\text{Mn}_{3/4}$ , is estimated to be  $4.65(2)\mu_B$  from the susceptibility data above 300 K and agrees well with  $4.72\mu_B$  calculated from the spin-only values for  $\text{Fe}^{3+}_{1/4}\text{Mn}^{3+}_{1/4}\text{Mn}^{4+}_{1/2}$  with high-spin configurations. Thus, from a combination of the Mössbauer spectrum and the magnetic susceptibility data, the charge distribution in the sample is most likely written as  $\text{Li}^+_{2}\text{Fe}^{3+}\text{Mn}^{3+}\text{Mn}^{4+}_2\text{O}_8$ .

A powder X-ray diffraction (XRD) pattern recorded with a Stoe Stadi/P diffractometer using  $\text{Cu K}\alpha_1$  radiation was indexed in the cubic space group  $Fd\bar{3}m$  with lattice parameter  $a = 8.2508(8)$  Å, revealing  $\text{Li}_2\text{FeMn}_3\text{O}_8$  as a phase-pure spinel (Figure 3). High fluorescence backgrounds, caused by an interaction between Fe/Mn and  $\text{Cu K}\alpha_1$  radiation allowed us to refine only the cation distribution by the Rietveld method with the pattern fitting structure refinement (PFSR) program in the Stoe software package. Various models with cations distributed differently on  $8a$  and  $16d$  sites were tested by generating theoretical XRD patterns, using the atomic positions of the spinel phase  $\text{Li}_4\text{Mn}_5\text{O}_{12}$ <sup>19</sup> with isotropic thermal parameters of 0.05 for all atomic positions, and several likely models were examined further by Rietveld analysis. The most probable model, with minimum  $R$  values,<sup>20</sup> was found to be  $\text{Li}_{8a}[\text{Fe}_{0.5}\text{Mn}_{1.5}]_{16d}\text{O}_4$ , i.e.,  $\text{Li}^+_{8a}[\text{Fe}^{3+}_{0.5}\text{Mn}^{3+}_{0.5}\text{Mn}^{4+}_{1.0}]_{16d}\text{O}_4$ : Li fully occupies tetrahedral  $8a$  sites; Fe and Mn are situated in octahedral  $16d$  sites with the molar ratio

1:3. Fe and Mn have very similar atomic scattering factors, and thus little information is obtainable from our XRD data about possible cation ordering<sup>21</sup> in octahedral sites; further structural study is in progress.

For electrochemical measurements, the positive electrode was made by blending the sample with 5 wt % acetylene black as an active material and 8 wt % polyvinylidene fluoride as a binder. A glass test cell consisted of the above composite positive electrode, Li metal foil as the negative electrode, Li metal as a reference, and 1 M  $\text{LiPF}_6$  dissolved in propylene carbonate as the electrolyte. The cell was cycled galvanostatically in the range 3.0–5.3 V vs  $\text{Li/Li}^+$ ; current density was fixed at  $0.5$  mA/cm<sup>2</sup> for charge, and discharge used varied current densities:  $0.5$  mA/cm<sup>2</sup> for cycles 1, 2, and 7–36,  $2.5$  mA/cm<sup>2</sup> for cycles 3 and 4, and  $5.0$  mA/cm<sup>2</sup> for cycles 5 and 6.

The potential profile during the first cycle is shown in Figure 4. Two reversible plateaux indicate two-step extraction/reinsertion of Li from/into the cathode material. The plateau centered at 4.1 V was observed previously,<sup>15</sup> but to our knowledge, the plateau centered at 4.9 V for discharge is reported here for the first time. The first charge shows a capacity of  $\sim 65$  mA h g<sup>-1</sup> at the plateau centered at 4.1 V. On converting the capacity to  $X$  in  $\text{Li}_{2-X}\text{FeMn}_3\text{O}_8$ ,  $X$  reaches  $\sim 0.88$  at the sharp transition point between the two plateaux. False charge capacity occurs at potentials higher than  $\sim 5.0$  V, owing to electrolyte oxidation, and is generally shown by a constant difference between each discharge capacity and the following recharge capacity.<sup>22</sup> In this case, the difference decreases gradually with cycling, however (Figure 5). After taking account of the electrolyte oxidation effect, the plateau centered at 5.0 V is found to have almost the same charge capacity as that of the plateau centered at 4.1 V, i.e.,  $\sim 65$  mA h g<sup>-1</sup>. The composition after charging to 5.3 V is then estimated to be  $\text{Li}_{0.24}\text{FeMn}_3\text{O}_8$ , indicating that  $\sim 12$  mol % Li still

(19) Takada, T.; Hayakawa, H.; Akiba, E. *J. Solid State Chem.* **1995**, *115*, 420.

(20) Rietveld, H. M. *J. Appl. Crystallogr.* **1969**, *2*, 65.

(21) Kawai, H.; Tabuchi, M.; Nagata, M.; Tukamoto, H.; West, A. R. *J. Mater. Chem.* **1998**, *8*, 1273.

(22) Kawai, H.; Nagata, M.; Tukamoto, H.; West, A. R. Unpublished data.

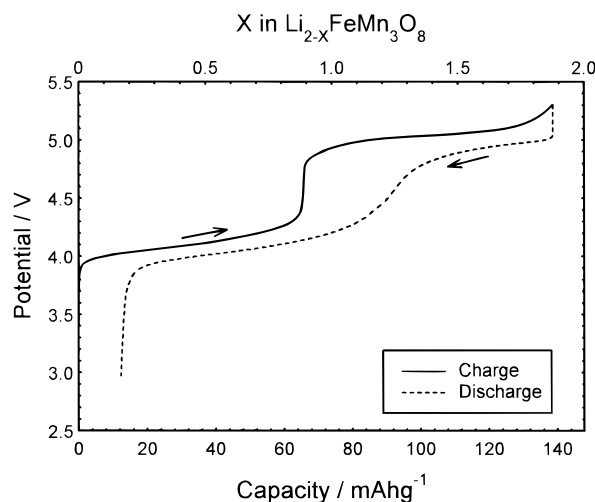


**Figure 4.** Potential profile during the first cycle for  $\text{Li}_{2-x}\text{FeMn}_3\text{O}_8$ .

remains inside the cathode material. All Li is situated in tetrahedral  $8a$  sites for  $\text{Li}_2\text{FeMn}_3\text{O}_8$ , and thus extraction appears to occur fully, through the well-known conduction pathway  $8a \rightarrow 16c \rightarrow 8a \rightarrow 16c$ , to a plausible end composition  $\text{Fe}^{4+}\text{Mn}^{4+}_3\text{O}_8$ . Improvement in electrolyte stability is needed to measure electrochemical properties at higher potentials.

The first discharge takes place initially at the high-voltage plateau centered at 4.9 V, with a capacity of  $\sim 50 \text{ mA h g}^{-1}$ , switching fairly gently to the plateau centered at 4.1 V, with capacity of  $\sim 75 \text{ mA h g}^{-1}$  (Figure 4). The discharge profile in fact starts from  $\sim 5.0 \text{ V}$ , and thus  $\text{Li}_2\text{FeMn}_3\text{O}_8$  may be called a 5 V cathode material. Two redox reactions appear to take place during cycling: (1)  $\text{Mn}^{3+}_{16d} \leftrightarrow \text{Mn}^{4+}_{16d}$ , (2)  $\text{Fe}^{3+}_{16d} \leftrightarrow \text{Fe}^{4+}_{16d}$ . The plateau centered at 4.1 V has been reported to originate from reaction 1 for several spinel compounds including  $\text{LiMn}_2\text{O}_4$ ,<sup>3,4</sup>  $\text{LiCr}_x\text{Mn}_{2-x}\text{O}_4$ ,<sup>14</sup> and  $\text{LiNi}_x\text{Mn}_{2-x}\text{O}_4$ .<sup>16,17</sup> It is thus likely that reaction 2, i.e.,  $\text{Fe}^{3+}_{16d} \leftrightarrow \text{Fe}^{4+}_{16d}$  is responsible for the plateau centered at 4.9 V. The

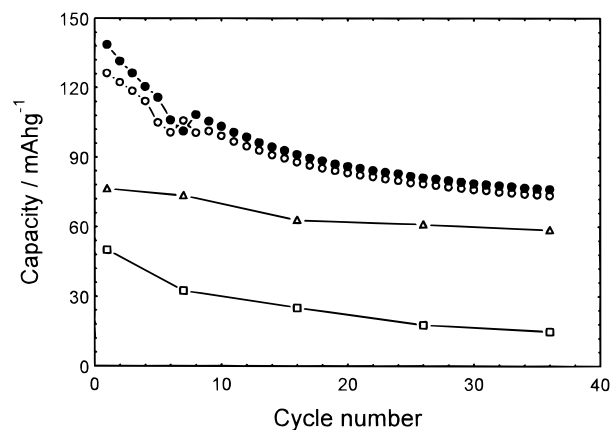


**Figure 5.** Variation in total charge (●) and discharge (○) capacity and specific discharge capacity of the plateau centered at 4.1 V (Δ) and the plateau centered at 4.9 V (□) upon cycling for  $\text{Li}_2\text{FeMn}_3\text{O}_8$  (○ = Δ + □).

plateau centered at 4.1 V shows good cyclability, maintaining its discharge capacity to well over 35 cycles (Figure 5). The plateau centered at 4.9 V changed its shape gradually with cycling, from a clear plateau to a hyperbolic slope (not shown) and exhibits fairly rapid capacity fading during the first six cycles, where current densities higher than  $0.5 \text{ mA/cm}^2$  were frequently used (Figure 5).

Discovery of the high-voltage plateau centered at 4.9 V gives  $\text{Li}_2\text{FeMn}_3\text{O}_8$  possible applications as a cathode material in high-voltage Li ion batteries. In comparison with  $\text{Li}_2\text{CoMn}_3\text{O}_8$ , it also offers potential economical and environmental advantages. Further work to improve the capacity and cycling performance of the plateau centered at 4.9 V is in progress.

**Acknowledgment.** H.K. thanks CVCP for an ORS Award. We acknowledge the assistance of H. Sakaebe for the  $^{57}\text{Fe}$  Mössbauer spectrum.

CM9807182